Scientific Research Publishing

Materials Sciences and Applications, 2020, 11, 744-756
https://www.scirp.org/journal/msa
ISSN Online: 2153-1188
ISSN Print: 2153-117X

Polycaprolactone (PCL) Chains Grafting on the Surface of Cellulose Nanocrystals (CNCs) during *In Situ* Polymerization of ε-Caprolactone at Room Temperature

Jérémy Astruc[1], Patrice Cousin[1], Gaétan Laroche[2,3], Mathieu Robert[1], Saïd Elkoun[1*]

[1]Center of Innovative Technology and Eco-Design (CITE), University of Sherbrooke, Granby, QC, Canada
[2]Laboratoire d'Ingénierie de Surface, Département de Génie des Mines, de la Métallurgie et des Matériaux Centre de recherche sur les Matériaux avancés, Pavillon Adrien-Pouliot, University of Laval, Québec, QC, Canada
[3]Centre de Recherche du CHU de Québec, Hôpital Saint-François d'Assise, Québec, QC, Canada

Email: *Said.Elkoun@Usherbrooke.ca

How to cite this paper: Astruc, J., Cousin, P., Laroche, G., Robert, M. and Elkoun, S. (2020) Polycaprolactone (PCL) Chains Grafting on the Surface of Cellulose Nanocrystals (CNCs) during *In Situ* Polymerization of ε-Caprolactone at Room Temperature. *Materials Sciences and Applications*, **11**, 744-756.
https://doi.org/10.4236/msa.2020.1111050

Received: August 27, 2020
Accepted: November 10, 2020
Published: November 13, 2020

Abstract

This work aimed at investigating the feasibility of surface modification of cellulose nanocrystals (CNCs) using *in situ* ring opening polymerization of ε-caprolactone (ε-CL) at room temperature. Residues of flax and milkweed *(Asclepias syriaca)* stem fibers were used as a source of cellulose to obtain and isolate CNCs. The cationic ring opening polymerization (CROP) of the monomer ε-CL was used to covalently graft polycaprolactone (PCL) chains at the CNCs surface. Silver hexafluoroantimonate ($AgSbF_6$) was used in combination with the extracted CNCs to initiate, at room temperature, the polymerization and the grafting reactions with no other stimulus. Fourier-Transform InfraRed (FTIR), X-ray Photoelectron Spectrometry (XPS), UV/visible absorption and Gel Permeation Chromatography (GPC) analyses evidenced the presence of PCL chains covalently grafted at CNCs surface, the formation of Ag(0) particles as well as low or moderate molecular weight free PCL chains.

Keywords

Cellulose Nanocrystals (CNCs), Simultaneous Polymerization and Surface Grafting, ε-Caprolactone, Cationic Ring Opening Polymerization, Room Temperature, Silver Hexafluoroantimonate

1. Introduction

Nowadays, environmental protection is one of the main concerns of our society.

It is well known that the omnipresence of petro-based materials significantly contributes to pollution. Thus, it is not surprising that cellulose, the most important and abundant natural biopolymer in nature, became the focus of many interests for many years [1]. In composite materials, the use of cellulose fibers has been extensively studied due to their renewability and interesting properties as compared to petro-sourced materials [2]. Unfortunately, natural fibers exhibit a low durability under certain circumstances such as high humidity and biodegradation, preventing their use at a larger scale for certain applications [3]. To overcome this problem, many studies focus on the use of cellulose nanocrystals (CNCs). Indeed and as compared to cellulosic fibers, CNCs are the crystalline parts of cellulose that present a better resistance to biodegradation and offer interesting properties for composite applications, such as large specific surface area and high stiffness [4].

Nevertheless, due to the hydrophilic nature of CNCs, their direct incorporation in hydrophobic matrices is not sufficient to provide a good interfacial adhesion and significantly increase the properties of composite materials [1]. As a consequence, numerous studies were aimed at chemically compatibilizing CNCs with various hydrophobic matrices using different approaches, such as silanization, esterification, acetylation, polymer grafting, etc. [5]. Among the investigated approaches, polymer grafting seems to be a promising way to compatibilize CNCs as it allows grafting polymer chains, partially or totally miscible with a specific polymer matrix, at CNCs surface [6]. The molecular weight of grafted chains is, however, a factor that greatly influences CNCs dispersion and interfacial adhesion with the matrix due to chain entanglements and cocrystallization [7]. It is also assumed that the higher the grafting density, the better the properties. However, according to literature, high-grafting density is mainly achieved using the "grafting from" method during *in situ* polymerization. The other possible grafting method usually referred to as "grafting onto" is based on the grafting of pre-polymerized chains at CNCs surface, which is generally restricted by steric hindrance occurring during the reaction [8]. Among the commercially available biopolymers, polycaprolactone (PCL) has drawn particular attention. PCL is a biodegradable polymer with moderate cost, good compatibility with other biopolymers, such as polylactic acid (PLA), low glass transition and melting temperatures (−60˚C and 60˚C, respectively). It offers interesting properties for diverse applications such as packaging, medicine and tissue engineering [9] [10] [11]. PCL is traditionally produced by Ring Opening Polymerization (ROP) of ε-caprolactone (ε-CL), a cyclic monomer, leading to high molecular weight chains and low polydispersities [10] [12]. This *in situ* polymerization can be driven for lactones, through hydroxyl groups present on the surface of cellulose fibers or CNCs [13].

ROP was intensively studied with lactones such as PCL or PLA for CNCs compatibilization by *in situ* grafting PCL or PLA chains at their surface. Different systems were studied, based on metal, radical, organic or enzymatic catalyst in different solvents or in bulk, generally at temperatures between

60˚C and 130˚C [7] [14]-[19]. The common system studied for PCL grafting by ROP at CNCs surface providing the most effective results is the use of tin(II)-2-ethylhexanoate ($Sn(Oct)_2$) as catalyst in toluene under heating, generally around 95˚C [8] [17]. However, this system, driven by a coordination-insertion mechanism, required external stimuli under inert atmosphere to avoid the degradation of the catalyst [13]. Moreover, this approach aimed at improving grafting density on CNCs surface and does not allow the grafting of CNCs and polymerization of PCL, simultaneously.

In that way, cationic ring opening polymerization (CROP) can occur under soft conditions, which offers an interesting alternative for atmospheric reaction and larger-scale production [12]. CROP is generally driven by the formation of reactive cationic intermediates, and as a result, requires less energy than other reactions [20]. However, the development of an efficient and simple system under soft conditions able to simultaneously initiate polymerization of free PCL chains and grafting of PCL chains on CNCs surface remains a challenge. Recently, Tehfe *et al.* reported that the use of silver hexafluoroantimonate salt ($AgSbF_6$) allowed the CROP reaction to take place at room temperature in the presence of oxygen or water, which generally act as inhibitors with other catalysts [21].

So far and to the best of the authors' knowledge, no report presents the use of silver hexafluoroantimonate salt ($AgSbF_6$) as a catalyst for the simultaneous PCL chains polymerization and grafting at CNCs surface through *in situ* CROP. In this paper, the CROP mechanism in presence of silver hexafluoroantimonate and CNCs derived from flax and milkweed stem fiber residues, is studied as well as the grafting of PCL chains on CNCs surface.

2. Experimental Part

2.1. Compounds

Flax stem fibers were provided by Biolin Research (Saskatoon, Canada) and milkweed stem fibers by producers from Saint Lawrence Valley, (Quebec, Canada). Toluene, dichloromethane, tetrahydrofuran (THF), sodium hydroxide, sodium bisulfite, sodium chlorite, sulfuric acid (98%), silver hexafluoroantimonate (V) ($AgSbF_6$), ε-caprolactone (ε-CL), polycaprolactone (PCL; M_n ~10,000 g/mol) and ethanol (95%) were purchased from Sigma-Aldrich (Ontario, Canada).

2.2. Cellulose Extraction

Pure cellulose type-II was extracted from flax and milkweed stem fibers. A four-step procedure described in detail in a previous study is summarized in **Figure 1** [22]. Briefly, fibers were grinded in a first step, to facilitate the extraction by destroying the lignocellulosic structure and obtain powder with a narrow particle size distribution. Then, the powder was placed in a Soxhlet extractor and cleaned with a 2:1 toluene/ethanol solution for 8 h to remove extractives (*i.e.* waxes, fat, pectin and minerals). A bleaching procedure was carried out by using

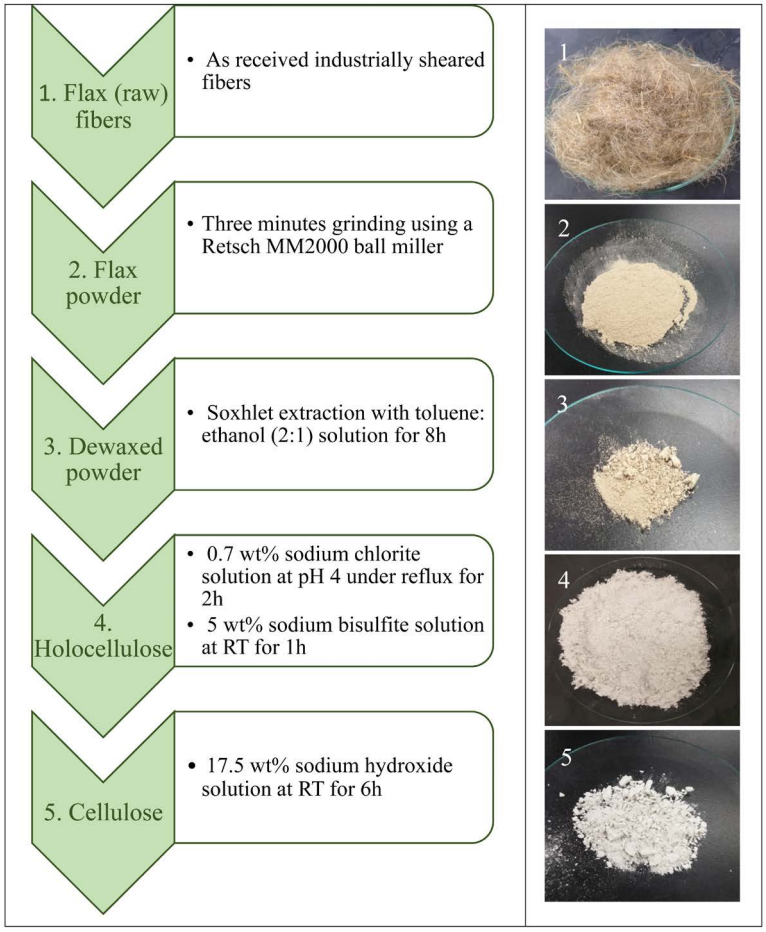

Figure 1. Procedure for pure cellulose type-II extraction from raw fibers.

a sodium chlorite solution under reflux and subsequently, a sodium bisulfite treatment at room temperature to remove lignin. Finally, hemicellulose was extracted while the crystalline structure of cellulose changed from native (cellulose-I) to mercerized cellulose (cellulose-II) using a 17.5 wt% NaOH solution at room temperature.

2.3. Isolation of Cellulose Nanocrystals

Cellulose-II was added in 64 wt% sulfuric acid (15 mL/g) at 57˚C during 140 min and, subsequently quenched in an ice bath. After washing by multiple centrifugation/redispersion cycles, dialysis was performed using distilled water to reach a neutral pH. The solution was finally filtered with a 4 - 5 μm glass filter and lyophilized.

2.4. Ring Opening Polymerization Procedure

CNCs and silver salt ($AgSbF_6$) were mixed with ε-CL monomers in a capped pillbox at room temperature for two days. A solid mixture consisting of PCL, CNCs and $AgSbF_6$ was obtained. CNCs were isolated after Soxhlet extraction in dichloromethane during 24 h to remove free PCL chains.

2.5. Characterization

FT-IR was carried out on commercial polycaprolactone, non-modified and modified CNCs using a JASCO 4600 spectrometer (Maryland, USA) equipped with an attenuated total reflectance (ATR) device. Spectra were obtained by accumulating 32 scans at a 4 cm^{-1} resolution for determining the formation of ester bonds between CNCs and PCL at 1720 cm^{-1}.

UV/visible measurements were carried out with a Spectra max plus 384 spectrometer (Connecticut, USA). The non-polymerized mixture was directly analyzed, whereas the polymerized material was previously crushed and dispersed in distilled water in order to visualise the formation of Ag(0) particles.

X-ray photoelectron spectrometry (XPS) measurements were performed using a KRATOS Axis Ultra XPS DLD (UK) equipped with an Al Kα monochromatic source (1486.6 eV) with applied power of 225 W. Non-modified and modified CNCs were analyzed in order to verify the grafting of PCL chains. The analyzer was operated in a constant pass energy mode (*PE* = 160 eV for the survey scans and *E*pass = 20 eV for the high resolution scans). The work function of the instrument was calibrated to give a binding energy (BE) of 83.96 eV for the 4f7/2 line of metallic Au. The dispersion of the spectrometer was adjusted to a BE of 932.63 eV for the 2p3/2 line of metallic Cu. A charge neutralizer was used on all samples to compensate for the charging effect. The samples were mounted on non-conductive adhesive tape to electrically isolate the sample and so, to avoid the differential charges effect. The charge corrections were done using the aliphatic carbon peak set at 285 eV. The analysed area was an oval of dimensions 300 x 700 µm. The Casa XPS software (version 2.3.18) was employed for data analysis, and the experimental Relative Sensitivity Factor (RSF) data as given by *Kratos Analytical* for their machines applied to quantify the XPS spectra. A Shirley background was utilized on all spectra.

Gel permeation chromatography (GPC) was used to determine the molecular weight (M_w) and number (M_n) of PCL free chains formed during the CROP. PCL was dissolved in THF and injected in a Waters 1515 HPLC (Ontario, Canada) equipped with a Waters model 2414 refractive index detector and a Waters Styragel HR0.5 column at a flow rate of 1 mL/min at 30˚C.

3. Results and Discussion

Reaction mechanism: $AgSbF_6$ and hydroxyl groups of CNCs were used as initiators and co-initiators, respectively, to simultaneously graft PCL on the surface of CNCs and formed free PCL macromolecules at room temperature. The mechanism of reaction proposed here consists of several steps: activation, initiation, propagation and termination (**Figure 2**). Briefly, in the activation step, $AgSbF_6$ acts as a Lewis acid and reacts with hydroxyl groups at the CNCs surface according to an alcohol reduction reaction that leads to the formation of carbonyl compounds, protons and Ag(0) particles (R.0) [23]. Then, the protons previously formed may react in two mechanisms, which leads to the formation

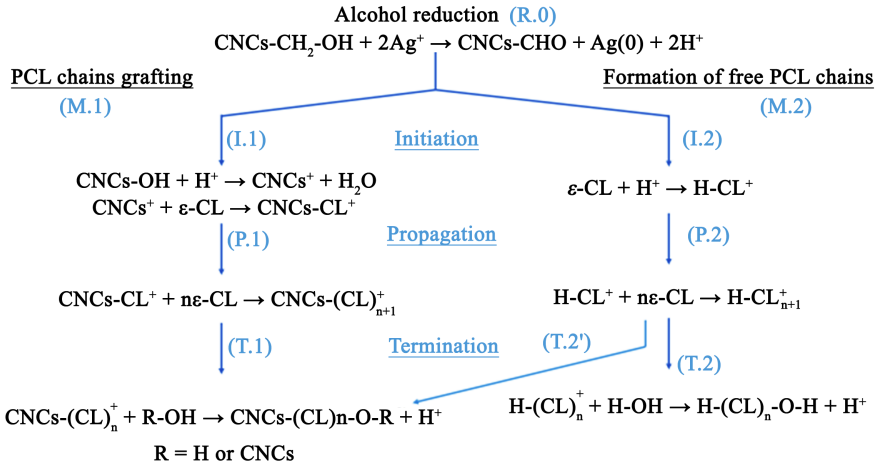

Figure 2. Reaction mechanisms of grafting PCL (M.1) and formation of free PCL (M.2) with $AgSbF_6$.

of grafted CNCs (M.1) and formation of free PCL (M.2). Initiation step with CNCs (I.1) and with *ε*-caprolactone (I.2) are followed by the propagation (P.1 and P.2) and termination (T.1 and T.2) steps [14].

This mechanism is supported by several studies showing that $H^+SbF_6^-$ and $RCH_2^+SBF_6^-$ are reactive species for the activation of *ε*-caprolactone and initiating cationic polymerization [21] [24]. However, it has to be noted that several secondary reactions may occur during the polymerization [20] [25]. To prevent these secondary reactions, it was shown that the counter-anion plays a crucial role in the polymerization mechanism [26]. Thus, by using a non-nucleophilic counter anion, such as SBF_6^-, the reactivity of cationic species is enhanced and the polymerization rate increased, whereas the secondary reactions are reduced [27].

After having reacted for 2 days, reactive systems with 5% $AgSbF_6$ were polymerized, whereas systems containing less than 2% $AgSbF_6$ remained non-polymerized (**Table 1**). The kinetic of polymerization is related to the amount of H^+ produced during the activation step by $AgSbF_6$ and depends on its concentration. However, even in the absence of CNCs, polymerization also occurs when 5 wt% $AgSbF_6$ is used. In this case, trace of humidity would react with silver salt and release H^+.

Formation of Ag(0) particles: Ag(0) particles are formed with the release of H^+ and their presence may be investigated by XPS and UV/visible spectroscopy to confirm the reaction mechanism suggested (**Figure 3** and **Figure 4**). XPS survey scans of non-modified and modified CNCs after Soxhlet extraction are shown in **Figure 3(a)**. Carbon and oxygen are the predominant elements. However, antimony and fluorine are evidenced in modified CNCs as well as silver from $AgSbF_6$. The high-resolution spectrum of Ag 3 d was further investigated (**Figure 3(b)**). Due to spin-orbit coupling, the signal of Ag 3 d is split into two peaks with an intensity ratio of 2/3, separated by a gap of 6.0 eV, that correspond to Ag 3 d 3/2 and Ag 3 d 5/2. Each peak is itself composed of two bands,

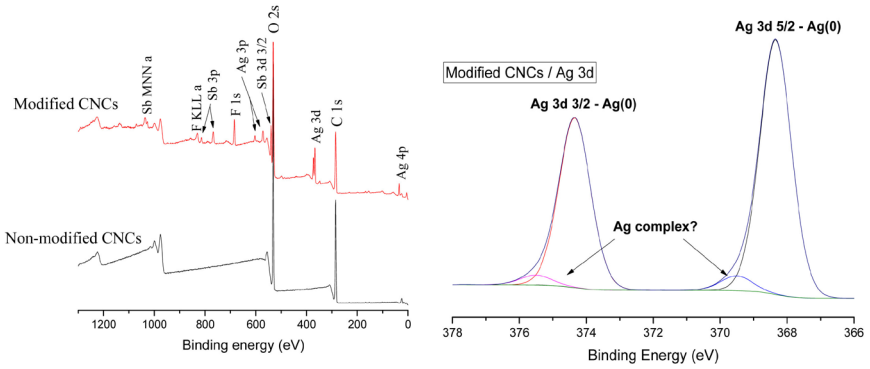

(a) (b)

Figure 3. (a) XPS wide scan of non-modified and modified CNCs; (b) Ag 3 d High-resolution and peaks deconvolution of modified CNCs.

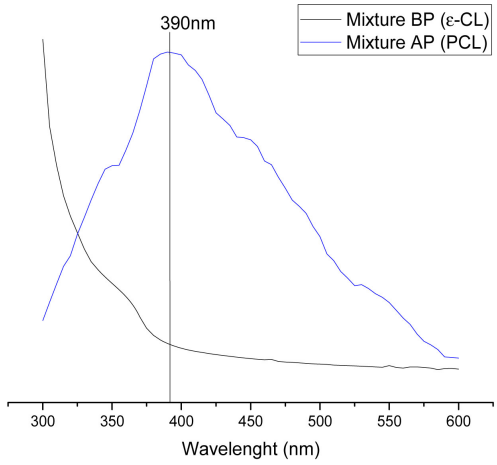

Figure 4. UV-visible absorption spectra of ε-CL/CNCs/$AgSbF_6$ system before (BP) and after polymerization (AP).

Table 1. Effect of CNCs and $AgSbF_6$ contents on CROP polymerization reaction.

CNCs (wt%)	$AgSbF_6$ (wt%)	After 2 days
-	1%	No Polymerization
-	2%	No Polymerization
-	5%	Polymerization. White color
5%	-	No polymerization
5%	2%	No polymerization
5%	5%	Polymerization. Tan color

one large and one small, corresponding to different Ag species. Concerning the Ag 3 d 5/2 peak, the large band located at a binding energy of 368.3 eV corresponds to the presence of Ag(0) particles, whereas the small band at 369.5 eV does not correspond to any known silver species in XPS tables [28]. However, several studies reported the presence of a similar XPS band possibly corresponding to silver complexation by carbonated species [29] [30] [31].

It is known that 20 nm silver nanoparticles absorb at 400 nm in the UV/visible spectrum [32]. Thus, the presence of Ag(0) particles generated during the CROP reaction may be investigated by UV/visible spectroscopy. **Figure 4** presents the spectrum of the ε-CL/CNCs/$AgSbF_6$ system before (BP) and after polymerization (AP). Before polymerization, the absorption rate is very large below 325 nm and reduced above 375 nm. A small shoulder close to 350 nm is also observed. This type of spectrum is characterized by cationic silver forming clusters [33]. After polymerization, a broad band around 390 nm appears, which can be related to spherical Ag(0) nanoparticles [34]. The broadening of this band may be accounted to a large size distribution and/or aggregation of Ag(0) particles, which may be explained by the acidic pH of the solution. Indeed, several authors have shown that the size of silver particles is inversely proportional to the pH [35]. It has to be noted that the presence of the shoulder around 350 nm corresponding to silver cluster is still detected after polymerization, which confirms the XPS results.

Grafting of PCL: PCL grafting on CNCs was investigated by FT-IR and XPS. Modified CNCs were previously purified by Soxhlet extraction in order to remove free adsorbed PCL [17]. Spectra of commercial PCL, non-modified and modified CNCs are reported in **Figure 5**. Spectra of non-modified and modified CNCs are quite similar, whereas modified CNCs present a specific band at 1722 cm^{-1}, related to C = O functions of PCL [36]. The intensity of this band is relatively low as compared to the one reported in other studies [17]. It may therefore be assumed that the grafting density is lower, which can be explained by the non-optimization of the process and use of freeze-drying for isolating CNCs leading to aggregate formation [36].

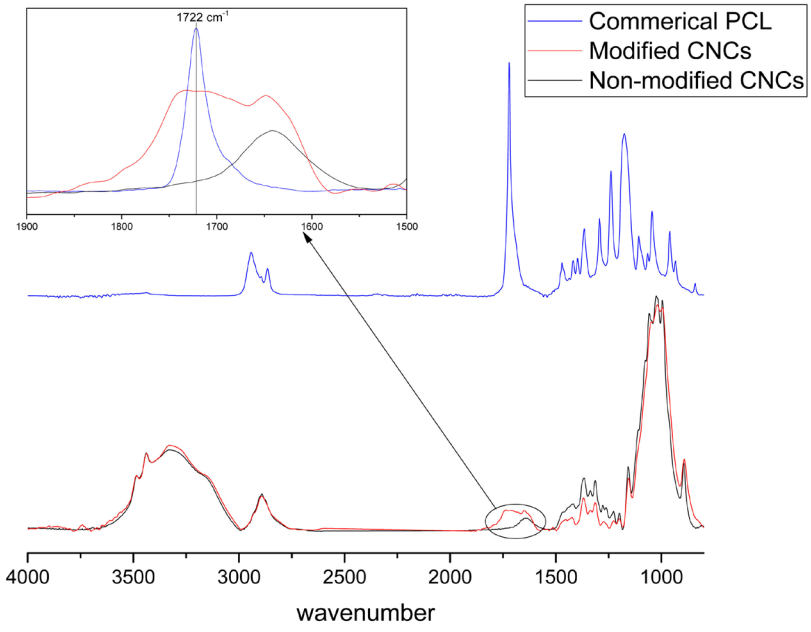

Figure 5. FT-IR spectra of commercial PCL, non-modified and modified CNCs. (PCL peak not at the same scale in the insert).

High resolution of the C 1s XPS spectra of non-modified and modified CNCs is reported in **Figure 6**. After curve fitting, both signals can be resolved in four bands, corresponding to the different environments of carbon atoms. The binding energies and ratios of these bands are presented in **Table 2**. Non-modified CNCs present a large contribution of C-O associated to the hydroxyl functions of cellulose (67.6% of total carbons) whereas 18.2% is attributed to O-C-O bonds corresponding to glycosidic linkage. This value is close to the theoretical value of 20% obtained by Habibi *et al.* for pure nanocellulose [6]. The bands at 289.6 eV and 285 eV correspond to ester/carboxylic groups and to aliphatic hydrocarbons respectively. Nevertheless, the presence of aliphatic compounds can only be explained by the presence of some byproducts and/or contaminants because pure cellulose does not contain these groups (Habibi *et al.*, 2008; Tian *et al.*, 2014). Comparatively, modified CNCs present lower C-O and O-C-O ratios, whereas C-C, C-H and COO proportions are larger (13.3% to 51.6% and 0.9% to 4.7%, respectively). This is due to the replacement of hydroxyl groups from CNCs by PCL which leads to the formation of ester and alkyl groups. These values are consistent with reported data for PCL grafting systems using external heating around 100˚C [8] [36].

***Molecular weight of free PCL*:** Additionally, the number (M_n) and weight (M_w) average molecular weights as well as the polydispersity index (PDI = M_w/M_n) of free PCL were determined by GPC (**Table 3**). The value of M_n is 11543 g·mol^{-1} which corresponds to a polymerization degree of 101. Moreover, a PDI value of 1.92 was calculated, which is in agreement with reported results on cationic polymerization [12]. It must be mentioned that the molecular weight of grafted PCL chains should be lower than the one of free PCL, because of the steric hindrance at CNCs surface that leads to less reactive hydroxyl groups as compared to the hydroxyl groups of water [18].

Table 2. Functional group ratios and band positions of the C 1s high-resolution XPS bands of non-modified and modified CNCs.

Type of bonds	Band Position (eV)		Non-Modified CNCs %total carbon	Modified CNCs %total carbon
	Non-Modified CNCs	Modified CNCs		
C-C, C-H	285	285	13.3	51.6
C-O	286.7	286.6	67.6	34.5
O-C-O	288.2	288.3	18.2	9.3
COO	289.6	289.3	0.9	4.7

Table 3. Mn, Mw, polydispersity index (PDI) and number average polymerization degree (DP_n) of the free chains of PCL after polymerization by GPC.

Monomer	$AgSbF_6$ (wt%)	CNCs (wt%)	*M*n (g·mol^{-1})	*M*w (g·mol^{-1})	PDI	DP_n
ε-CL	5%	5%	11,543	22,138	1.92	101

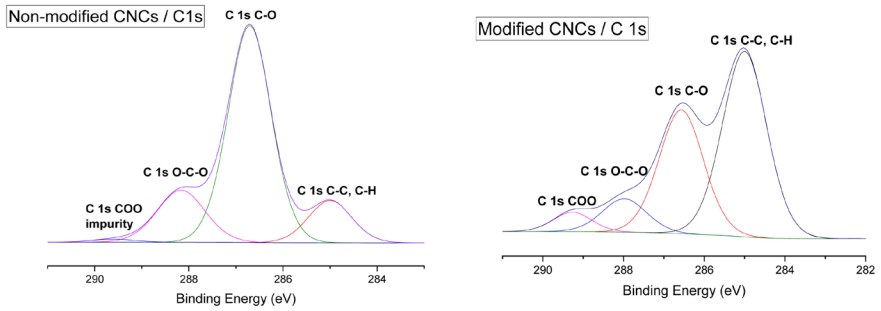

Figure 6. C 1s high-resolution XPS spectra of non-modified and modified CNCs.

4. Conclusion

This study highlighted that, simultaneous PCL polymerization and grafting at CNCs surface through *in situ* CROP at room temperature are possible thanks to the presence of $AgSbF_6$ and CNCs that act as initiator and co-initiator respectively. The resulting material is composed of free PCL, PCL-grafted CNCs, Ag(0) and impurities mainly related to the counter-anion (SbF_6^-). The formation of polydispersed Ag(0) particles, leading to the release of protons initiating the polymerization of PCL, was evidenced by UV/visible and XPS analysis. Moreover, PCL grafting on CNCs was confirmed by XPS and FT-IR. The significant increase of the C-C, C-H ratios observed by XPS, as well as M_n, M_w and DP_n values, obtained by GPC for free PCL suggest promising results for CROP at room temperature, once the procedure optimized.

Acknowledgements

The authors would like to thank the National Science and Engineering Research Council (NSERC) of Canada, the Centre Québécois sur les Matériaux Fonctionnels (CQMF) du Fonds de Recherche du Québec: Nature et Technologies (FRQNT) and the Consortium de Recherche et Innovations en Bioprocédés Industriels du Québec (CRIBIQ) for financial support. The authors are grateful to Dr. Mohamad Ali Tehfe and Sonia Blais for their technical assistance.

Conflicts of Interest

The authors declare no conflicts of interest regarding the publication of this paper.

References

[1] Habibi, Y., Lucia, L.A. and Rojas, O.J. (2010) Cellulose Nanocrystals: Chemistry, Self Assembly, and Applications. *Chemical Reviews*, **110**, 3479-3500. https://doi.org/10.1021/cr900339w

[2] Kalia, S., Dufresne, A., Cherian, B.M., Kaith, B.S., Avérous, L., Njuguna, J. and Nassiopoulos, E. (2011) Cellulose-Based Bio- and Nanocomposites: A Review. *International Journal of Polymer Science*, **2011**, Article ID: 837875. https://doi.org/10.1155/2011/837875

[3] Thakur, V.K. and Singha, A.S. (2010) KPS-Initiated Graft Copolymerization onto

Modified Cellulosic Biofibers. *International Journal of Polymer Analysis and Characterization*, **15**, 471-485. https://doi.org/10.1080/1023666X.2010.510294

[4] Moon, R.J., Martini, A., Nairn, J., Simonsen, J. and Youngblood, J. (2011) Cellulose Nanomaterials Review: Structure, Properties and Nanocomposites. *Chemical Society Reviews*, **40**, 3941. https://doi.org/10.1039/c0cs00108b

[5] Peng, B.L., Dhar, N., Liu, H.L. and Tam, K.C. (2011) Chemistry and Applications of Nanocrystalline Cellulose and Its Derivatives: A Nanotechnology Perspective. *The Canadian Journal of Chemical Engineering*, **89**, 1191-1206. https://doi.org/10.1002/cjce.20554

[6] Habibi, Y. and Dufresne, A. (2008) Highly Filled Bionanocomposites from Functionalized Polysaccharide Nanocrystals. *Biomacromolecules*, **9**, 1974-1980. https://doi.org/10.1021/bm8001717

[7] Goffin, A.-L., Raquez, J.-M., Duquesne, E., Siqueira, G., Habibi, Y., Dufresne, A. and Dubois, P. (2011) From Interfacial Ring-Opening Polymerization to Melt Processing of Cellulose Nanowhisker-Filled Polylactide-Based Nanocomposites. *Biomacromolecules*, **12**, 2456-2465. https://doi.org/10.1021/bm200581h

[8] Habibi, Y., Goffin, A.-L., Schiltz, N., Duquesne, E., Dubois, P. and Dufresne, A. (2008) Bionanocomposites Based on Poly(ε-caprolactone)-Grafted Cellulose Nanocrystals by Ring-Opening Polymerization. *Journal of Materials Chemistry*, **18**, 5002. https://doi.org/10.1039/b809212e

[9] Diaz, C.A., Pao, H.Y. and Kim, S. (2016) Film Performance of Poly(lactic acid) Blends for Packaging Applications. *Journal of Applied Packaging Research*, **8**, 4.

[10] Sisson, A.L., Ekinci, D. and Lendlein, A. (2013) The Contemporary Role of ε-Caprolactone Chemistry to Create Advanced Polymer Architectures. *Polymer*, **54**, 4333-4350. https://doi.org/10.1016/j.polymer.2013.04.045

[11] Ulery, B.D., Nair, L.S. and Laurencin, C.T. (2011) Biomedical Applications of Biodegradable Polymers. *Journal of Polymer Science Part B: Polymer Physics*, **49**, 832-864. https://doi.org/10.1002/polb.22259

[12] Kunioka, M., Wang, Y. and Onozawa, S. (2003) Polymerization of Poly(ε-caprolactone) Using Yttrium Triflate. *Polymer Journal*, **35**, 422. https://doi.org/10.1295/polymj.35.422

[13] Carlmark, A., Larsson, E. and Malmström, E. (2012) Grafting of Cellulose by Ring-Opening Polymerisation—A Review. *European Polymer Journal*, **48**, 1646-1659. https://doi.org/10.1016/j.eurpolymj.2012.06.013

[14] Labet, M. and Thielemans, W. (2011) Improving the Reproducibility of Chemical Reactions on the Surface of Cellulose Nanocrystals: ROP of ε-Caprolactone as a Case Study. *Cellulose*, **18**, 607-617. https://doi.org/10.1007/s10570-011-9527-x

[15] Lin, N., Chen, G., Huang, J., Dufresne, A. and Chang, P.R. (2009) Effects of Polymer-Grafted Natural Nanocrystals on the Structure and Mechanical Properties of Poly(lactic acid): A Case of Cellulose Whisker-Graft-Polycaprolactone. *Journal of Applied Polymer Science*, **113**, 3417-3425. https://doi.org/10.1002/app.30308

[16] Lizundia, E., Fortunati, E., Dominici, F., Vilas, J.L., León, L.M., Armentano, I. and Kenny, J.M. (2016) PLLA-Grafted Cellulose Nanocrystals: Role of the CNC Content and Grafting on the PLA Bionanocomposite Film Properties. *Carbohydrate Polymers*, **142**, 105-113. https://doi.org/10.1016/j.carbpol.2016.01.041

[17] Lönnberg, H., Zhou, Q., Brumer, H., Teeri, T.T., Malmström, E. and Hult, A. (2006) Grafting of Cellulose Fibers with Poly(ε-caprolactone) and Poly(lactic acid) via Ring-Opening Polymerization. *Biomacromolecules*, **7**, 2178-2185. https://doi.org/10.1021/bm060178z

[18] Miao, C. and Hamad, W.Y. (2016) *In-Situ* Polymerized Cellulose Nanocrystals (CNC) Poly(l-lactide) (PLLA) Nanomaterials and Applications in Nanocomposite Processing. *Carbohydrate Polymers*, **153**, 549-558. https://doi.org/10.1016/j.carbpol.2016.08.012

[19] Peltzer, M., Pei, A., Zhou, Q., Berglund, L. and Jiménez, A. (2014) Surface Modification of Cellulose Nanocrystals by Grafting with Poly(lactic acid): Surface Modification of Cellulose Nanocrystals. *Polymer International*, **63**, 1056-1062. https://doi.org/10.1002/pi.4610

[20] Peacock, A.J. and Calhoun, A.R. (2006) Polymer Chemistry: Properties and Applications. Hanser Gardner Publications, Munich. https://doi.org/10.3139/9783446433434

[21] Tehfe, M.-A., Jamois, R., Cousin, P., Elkoun, S. and Robert, M. (2015) *In Situ* Synthesis and Characterization of Silver/Polymer Nanocomposites by Thermal Cationic Polymerization Processes at Room Temperature: Initiating Systems Based on Organosilanes and Starch Nanocrystals. *Langmuir*, **31**, 4305-4313. https://doi.org/10.1021/la504518c

[22] Astruc, J., Nagalakshmaiah, M., Laroche, G., Grandbois, M., Elkoun, S. and Robert, M. (2017) Isolation of Cellulose-II Nanospheres from Flax Stems and Their Physical and Morphological Properties. *Carbohydrate Polymers*, **178**, 352-359. https://doi.org/10.1016/j.carbpol.2017.08.138

[23] El-Sheikh, M.A. (2014) A Novel Photosynthesis of Carboxymethyl Starch-Stabilized Silver Nanoparticles. *The Scientific World Journal*, **2014**, Article ID: 514563. https://doi.org/10.1155/2014/514563

[24] Crivello, J.V., Dietliker, K. and Bradley, G. (1999) Photoinitiators for Free Radical Cationic & Anionic Photopolymerisation. Wiley, Hoboken.

[25] Farrell, D.J., McArdle, C., Doherty, M. and Kelly, J.M. (2012) Surface Promoted Redox Cationic Polymerization of Epoxy Monomers Catalyzed by Silver Salts. *Journal of Polymer Science Part A*: *Polymer Chemistry*, **50**, 2957-2966. https://doi.org/10.1002/pola.26082

[26] Yağci, Y. and Reetz, I. (1998) Externally Stimulated Initiator Systems for Cationic Polymerization. *Progress in Polymer Science*, **23**, 1485-1538. https://doi.org/10.1016/S0079-6700(98)00010-0

[27] Ortyl, J. and Popielarz, R. (2012) New Photoinitiators for Cationic Polymerization. *Polimery*, **57**, 510-517. https://doi.org/10.14314/polimery.2012.510

[28] Nehlig, E., Schneider, R., Vidal, L., Clavier, G. and Balan, L. (2012) Silver Nanoparticles Coated with Thioxanthone Derivative as Hybrid Photoinitiating Systems for Free Radical Polymerization. *Langmuir*, **28**, 17795-17802. https://doi.org/10.1021/la303923p

[29] Biniak, S., Pakula, M. and Światkowski, A. (1999) Influence of Surface Chemical Structure of Active Carbon on Its Electrochemical Behaviour in the Presence of Silver. *Journal of Applied Electrochemistry*, **29**, 481-487. https://doi.org/10.1023/A:1003424419533

[30] Bootharaju, M.S. and Pradeep, T. (2010) Uptake of Toxic Metal Ions from Water by Naked and Monolayer Protected Silver Nanoparticles: An X-Ray Photoelectron Spectroscopic Investigation. *The Journal of Physical Chemistry C*, **114**, 8328-8336. https://doi.org/10.1021/jp101988h

[31] Macková, A., Švorčík, V., Sajdl, P., Strýhal, Z., Pavlík, J., Malinský, P. and Šlouf, M. (2007) RBS, XPS, and TEM Study of Metal and Polymer Interface Modified by Plasma Treatment. *Vacuum*, **82**, 307-310.

https://doi.org/10.1016/j.vacuum.2007.07.027

[32] Saion, E., Gharibshahi, E. and Naghavi, K. (2013) Size-Controlled and Optical Properties of Monodispersed Silver Nanoparticles Synthesized by the Radiolytic Reduction Method. *International Journal of Molecular Sciences*, **14**, 7880-7896. https://doi.org/10.3390/ijms14047880

[33] Balavandy, S., Shameli, K., Biak, D.R.B.A. and Abidin, Z. (2014) Stirring Time Effect of Silver Nanoparticles Prepared in Glutathione Mediated by Green Method. *Chemistry Central Journal*, **8**, 11. https://doi.org/10.1186/1752-153X-8-11

[34] Rauwel, P., Rauwel, E., Ferdov, S. and Singh, M.P. (2015) Silver Nanoparticles: Synthesis, Properties, and Applications. *Advances in Materials Science and Engineering*, **2015**, Article ID: 624394. https://doi.org/10.1155/2015/624394

[35] Alqadi, M.K., Abo Noqtah, O.A., Alzoubi, F.Y., Alzouby, J. and Aljarrah, K. (2014) pH Effect on the Aggregation of Silver Nanoparticles Synthesized by Chemical Reduction. *Materials Science-Poland*, **32**, 107-111. https://doi.org/10.2478/s13536-013-0166-9

[36] Tian, C., Fu, S., Chen, J., Meng, Q. and Lucia, L.A. (2014) Graft Polymerization of Epsilon-Caprolactone to Cellulose Nanocrystals and Optimization of Grafting Conditions Utilizing a Response Surface Methodology. *Nordic Pulp & Paper Research Journal*, **29**, 58-68. https://doi.org/10.3183/npprj-2014-29-01-p058-068